A. Kuzmin, A. Anspoks, A. Kalinko, J. Timoshenko, L. Nataf, F. Baudelet, T. Irifune,
Origin of pressure-induced metallization in Cu3N: an X-ray absorption spectroscopy study,
Phys. Status Solidi B 255 (2018) 1800073:1-6.

physica status solidi

Origin of Pressure-Induced Metallization in Cu_3N: an X-ray Absorption Spectroscopy Study

A. Kuzmin[*,1], A. Anspoks[1], A. Kalinko[2], J. Timoshenko[3], L. Nataf[4], F. Baudelet[4], T. Irifune[5]

[1] Institute of Solid State Physics, University of Latvia, Kengaraga street 8, LV-1063 Riga, Latvia

[2] Department Chemie, Naturwissenschaftliche Fakultät, Universität Paderborn, Warburger Straße 100, 33098, Paderborn, Germany

[3] Department of Materials Science and Chemical Engineering, Stony Brook University, NY, 11794, USA

[4] Synchrotron SOLEIL, l'Orme des Merisiers, Saint-Aubin 91190, France

[5] Geodynamics Research Center, Ehime University, 2-5 Bunkyo-cho, Matsuyama, Ehime 790-8577, Japan

Key words: Cu_3N, Cu K-edge, XANES, EXAFS, high-pressure

[*] Corresponding author: e-mail a.kuzmin@cfi.lu.lv

High-pressure (0–26.7 GPa) Cu K-edge X-ray absorption spectroscopy was used to study possible structural modifications of anti-perovskite-type copper nitride (Cu_3N) crystal lattice. The analysis of X-ray absorption near-edge structure (XANES) and extended X-ray absorption fine structure (EXAFS), based on theoretical full-multiple-scattering and single-scattering approaches, respectively, suggests that at all pressures the local atomic structure of Cu_3N remains close to that in cubic $Pm\bar{3}m$ phase. Therefore, the transition to metal state above 5 GPa, observed previously using pressure-dependent electrical resistance and optical absorption measurements, is explained by the band gap collapse due to a decrease of the unit cell volume. We found that the lattice parameter of Cu_3N is reduced by $\sim$2% upon increasing pressure up to 26.7 GPa, and the structure is restored upon pressure release.

Copyright line will be provided by the publisher

A. Kuzmin, A. Anspoks, A. Kalinko, J. Timoshenko, L. Nataf, F. Baudelet, T. Irifune,
Origin of pressure-induced metallization in Cu3N: an X-ray absorption spectroscopy study,
Phys. Status Solidi B 255 (2018) 1800073:1-6.

1. Introduction

Studies of structural phase transitions driven by pressure play an important role in materials science and geosciences.[1,2] Recent developments in the field have been made possible by coupling diamond anvil cells (DACs) with synchrotron radiation based techniques[3,4] as well as due to advances in first principles calculations.[5–7] X-ray diffraction (XRD),[8,9] being sensitive to long range-order, and X-ray absorption spectroscopy (XAS),[10–12] giving element-specific information on the local electronic and atomic structures, are two complementary direct structural methods which are most often used to probe high-pressure structure transformations.

When a crystalline material suffers high-pressure load, a broadening of diffraction peaks may occur due to crystallites size reduction and an appearance of the local strain (microstrain) at the contact points between crystal grains.[13] Pressure-induced amorphization is also observed in many materials.[14] A significant broadening of the diffraction peaks can make ambiguous the precise analysis of the diffraction pattern and, as a result, the identification of the high-pressure phase. In this situation, the use of XAS can be beneficial, in particular, when the local environment around the absorbing atom in the low- and high-pressure phases is sufficiently different.

In this study, we will discuss the case of copper nitride (Cu_3N), which finds applications in optical storage media,[15,16] optical lithography/metallization layers,[17] resistive random-access memory (ReRAM),[18] spintronic devices,[19] for solar energy conversion,[20] and as a conductive ink.[21]

Cu_3N crystallizes at ambient pressure and temperature in anti-perovskite-type cubic crystal structure (also known as anti-ReO_3-type) built up of corner-sharing NCu_6 octahedra (Figure 1).[22,23] Opposite to perovskites, light anion (N) is located in Cu_3N at the octahedron centre occupying Wyckoff position 1a (0,0,0), whereas six metal cations (Cu) form regular octahedron and reside on Wyckoff position 3d (1/2,0,0).

The peculiarity of the Cu_3N crystal lattice is the presence of an empty space between eight NCu_6 octahedra located at the cube corners (Figure 1). Such crystal lattice and its low decomposition temperature (600–800 K[24–27]) indicate on the possibility of the Cu_3N structure instability under high pressure. In fact, the pressure-induced metallization of Cu_3N above $\sim$5 GPa has been observed in the past by electrical resistance[28] and optical absorption[29] measurements. However, its origin remains a puzzling

A. Kuzmin, A. Anspoks, A. Kalinko, J. Timoshenko, L. Nataf, F. Baudelet, T. Irifune,
Origin of pressure-induced metallization in Cu3N: an X-ray absorption spectroscopy study,
Phys. Status Solidi B 255 (2018) 1800073:1-6.

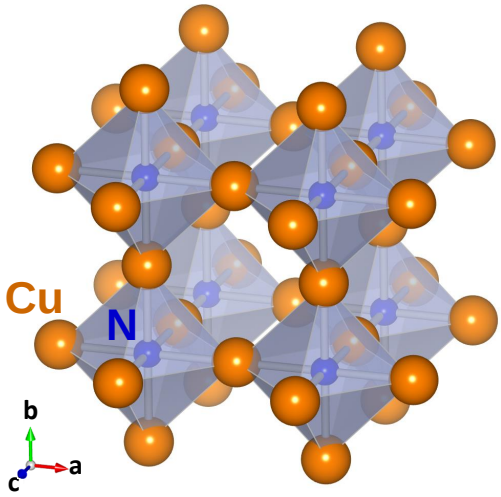

Figure 1 Crystal structure of cubic Cu_3N (space group $Pm\bar{3}m$ (221)) composed of regular NCu_6 octahedra.

task. X-ray[29,30] and neutron[29] diffraction data suggest the existence of the phase transition between 5 and 10 GPa from low-pressure $Pm\bar{3}m$ phase to high-pressure $I4/mmm$[29] or $P4/mmm$[30] phase. At the same time, available first principles calculations predict in Cu_3N a transition to several different phases[31,32] or even the absence of any structural transition up to 30 GPa.[33]

We have shown recently that XAS is well suited to probe the local environment of Cu_3N, providing detailed information on the thermal disorder and vibrational correlations.[34–36] Here we present the results of the room-temperature pressure-dependent (up to 26.7 GPa) Cu K-edge XAS study of Cu_3N. Theoretical simulations of the experimental data allowed us to validate the available structural models[28,31–33] and suggest that the metallic state in Cu_3N is reached under high pressure because of a continuous decrease and eventual collapse of the band gap.

2. Experimental Section

Our polycrystalline Cu_3N (Alfa Aesar, 99.5% purity) sample was characterized by X-ray diffraction at room-temperature using the Bruker AXS D2 PHASER benchtop Bragg-Brentano θ/θ powder diffractometer equipped with the LynxEye detector and copper anode (Cu Kα) tube. The sample was rotated during the measurement, and the pattern was collected in the angular range 2θ from 10° to 90° with the step of $\Delta(2\theta)$=0.04°.

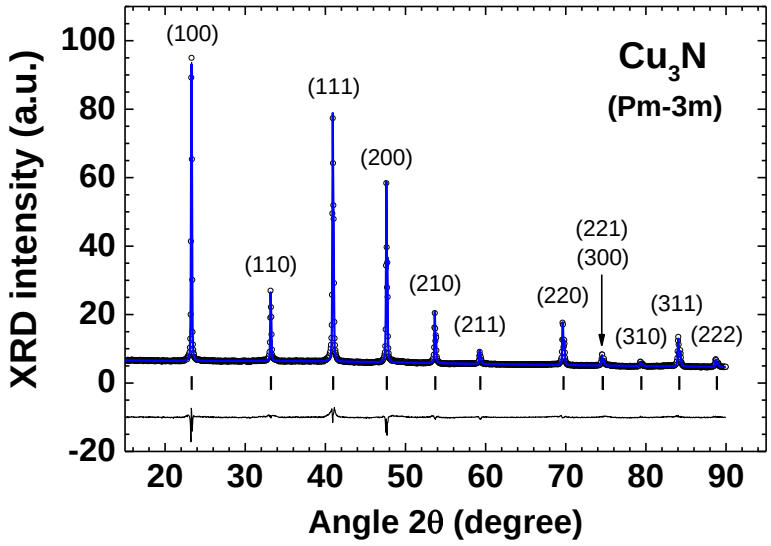

Figure 2 Rietveld refinement of the powder X-ray diffraction pattern of Cu_3N. Observed data points are indicated by open circles, the best-fit profile (upper curve) and the difference pattern (lower curve) are shown by solid lines. Vertical bars indicate the position of Bragg peaks for the $Pm\bar{3}m$ phase. The plane indices are also given.

Room-temperature pressure-dependent XAS was performed at the Cu K-edge using the dispersive set-up of the bending-magnet SOLEIL ODE beamline.[37] The SOLEIL synchrotron was operated in the top-up mode at energy of 2.75 GeV and current of 450 mA. The X-ray synchrotron radiation, produced by bending magnet, was dispersed and focused by a cooled single-crystal Si(111) polychromator bent in four points under vacuum. The focus spot size at the sample was about 30 μm FWHM. Two mirrors installed before and after the polychromator were used for a harmonic rejection. The X-ray absorption spectra were detected by a Princeton Instruments PIXIS-400 CCD camera coupled with a scintillator.

The sample pressure was controlled in the range of 0–26.7 GPa using a membrane-type nano-polycrystalline diamond anvil cell (NDAC).[12,38] The silicon oil was used as a pressure transmitting media, and the pressure in the cell was determined using ruby luminescence method.[39]

3. Data Analysis

Phase purity of polycrystalline Cu_3N sample was confirmed by the analysis of the X-ray powder diffraction pattern using the Rietveld method, implemented in the PROFEX code.[40] The result of the Rietveld refinement is shown in Figure 2. The obtained R-factors are R_{wp}=2.19% and R_{exp}=1.5%, and the goodness-of-fit χ^2=2.13.

A. Kuzmin, A. Anspoks, A. Kalinko, J. Timoshenko, L. Nataf, F. Baudelet, T. Irifune,
Origin of pressure-induced metallization in Cu3N: an X-ray absorption spectroscopy study,
Phys. Status Solidi B 255 (2018) 1800073:1-6.

The X-ray absorption spectra at the Cu K-edge were analysed using the EDA software package[41] following conventional procedure.[42] Firstly, the X-ray absorption near-edge structure (XANES) and extended X-ray absorption fine structure (EXAFS) were extracted from the experimental data. Next, the Fourier transforms (FTs) of the EXAFS spectra $\chi(k)k^2$ (k is the photoelectron wavenumber) were calculated using the 10%-Gaussian window function: they were not corrected for the backscattering phase shift of atoms, therefore the positions of all peaks are displaced to smaller distances relative to their crystallographic values.

The Cu K-edge XANES spectra of different Cu_3N phases were calculated accounting for electric dipolar and quadrupolar transitions by the *ab initio* FDMNES code[43,44] using full-multiple-scattering (FMS) approach (Green formalism) and a self-consistent muffin-tin potential. The phase structures were taken from the models reported in Refs.[28,31–33] . The real energy-dependent exchange-correlation correction was described by the Hedin-Lundqvist[45,46] potential. The calculated XANES was broadened using the convolution with a Lorentzian to account for the core-hole and the final state life-time.[44]

The Cu K-edge EXAFS $\chi(k)$ was analysed within the single-scattering approximation. The photoelectron wavenumber k is defined as $k = \sqrt{2m(E - E_0)}/\hbar$, where m is the electron mass, $\hbar$ is Plank's constant, E is the X-ray photon energy, and the threshold energy E_0=8982 eV defines the origin of the photoelectron kinetic energy. The least-square curve fitting of EXAFS spectra was performed in the k-space range from 1.5 to 7.5 Å^{-1} for a cluster resembling a fragment of the Cu_3N structure with the $Pm\bar{3}m$ symmetry and containing six coordination shells around absorbing copper atom. Due to a short k-space range, we have constrained the values of coordination numbers at crystallographic values, whereas the interatomic distances, related to the coordination shell radii, and the mean-square relative displacement (MSRD) factors were used as free parameters.[42] The required scattering amplitudes and phase shifts were calculated by the *ab initio* FEFF9 code[47,48] based on a self-consistent muffin-tin potential. The complex energy-dependent exchange-correlation Hedin-Lundqvist[45,46] potential was used to account for inelastic effects in FEFF9 calculations.

4. Results and Discussion

The cubic lattice parameter of our polycrystalline Cu_3N sample obtained by Rietveld refinement at

A. Kuzmin, A. Anspoks, A. Kalinko, J. Timoshenko, L. Nataf, F. Baudelet, T. Irifune,
Origin of pressure-induced metallization in Cu3N: an X-ray absorption spectroscopy study,
Phys. Status Solidi B 255 (2018) 1800073:1-6.

room-temperature and ambient pressure (Figure 2) is equal to 3.8167(1) Å. This value agrees well with those in previous studies: 3.819(1) Å,[23] 3.817(5) Å[30] and 3.811–3.820 Å.[49]

In situ X-ray absorption spectra were recorded at the Cu K-edge in the pressure range of 0-26.7 GPa (Figure 3(a)). As one can see, a change of the spectra shape upon pressure increase is rather small, and the position of the absorption threshold remains at the same energy of ∼8982 eV (Figure 3(b)). The pressure-dependence of the edge position at the half-height of the normalized Cu K-edge jump is shown in Figure 4: its qualitative behavior with the onset at ∼5 GPa correlates well with a transition to metal state observed in Refs.[28,29] .

In Figure 5 we compare a set of the Cu K-edge XANES spectra of Cu_3N, recorded at pressures from 0 to 26.7 GPa, with the XANES spectra of two reference samples – metallic copper (Cu^0) foil and $Cu^{2+}O$ powder. A strong difference between the XANES spectra of the three compounds is clearly visible. Moreover, a shift of the pre-edge shoulder occurs from 8979 eV in metallic copper to 8982 eV in Cu_3N and, finally, to 8984 eV in CuO as denoted with the horizontal arrow. It is caused by the difference in the oxidation state of copper ions in the three compounds. At the same time, the position of the pre-edge shoulder in Cu_3N remains unchanged at ∼8982 eV upon compression as well as after pressure release. This fact is in agreement with the copper oxidation state of $+1$ in Cu_3N. Note that the pre-edge shoulder in Cu_3N is due to the electron transition from 1s(Cu) level to the bottom of conduction band composed of 3d(Cu) and 2p(N) states with some small admixture of 4p(Cu) states.[50]

The results of the full-multiple-scattering calculations by the FDMNES code for different Cu_3N phases proposed in previous theoretical[31–33] and experimental[29,30] studies are shown in Figure 6. The experimental XANES spectra at two extreme pressures (0 and 26.7 GPa) are also presented for comparison. As one can see, only XANES for cubic $Pm\bar{3}m$ (221) phase agrees well with our experimental data and is able to reproduce four main features (A-D) as seen in Figure 6a. Both tetragonal phases $P4/mmm$ (123) and $I4/mmm$ (139) give XANES spectra which differ significantly in the range of peaks A-C with the experimental ones. The XANES spectra corresponding to other four phases, cubic Cu_3Au-type, hexagonal Li_3P-type (194), trigonal α-UO_3-type (164) and orthorhombic I-K_3N-type (63), also deviate significantly from our experimental data as seen in Figure 6b. To conclude, the FMS

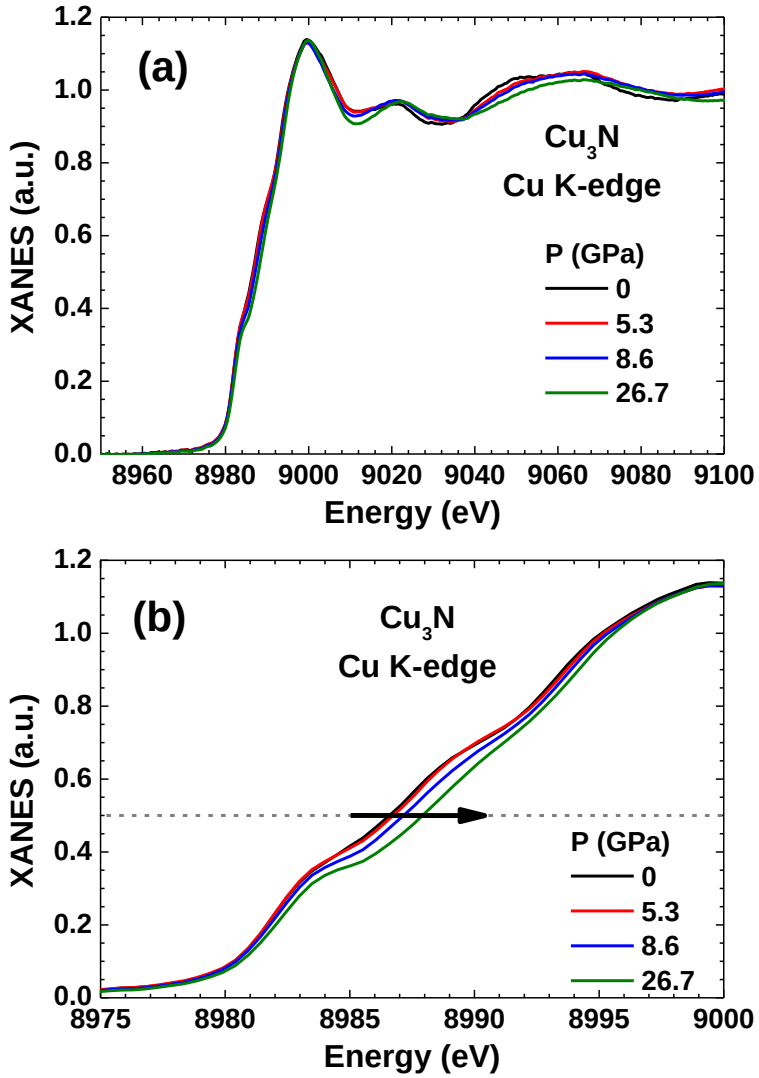

Figure 3 (a) Pressure-dependence of the Cu K-edge XANES of Cu_3N. (b) Enlarged region of the XANES close to the absorption edge. A change of the edge position at the half-height of the normalized Cu K-edge jump is indicated by the arrow.

simulations of the Cu K-edge XANES of Cu_3N suggest that cubic $Pm\bar{3}m$ (221) phase remains stable in the range of 0–26.7 GPa.

The experimental XANES spectra in Figure 3 can be also used to estimate the lattice parameter variation in Cu_3N upon compression using Natoli's rule.[52] The rule states that for solids of the same structure-type, the energy position of XANES peaks above the threshold (E_0) is inversely proportional to interatomic distance or lattice parameter: $(E - E_0 + \Delta E)(R - \Delta R)^2 = (E - E_0)R^2 = \text{const}$.[52] Therefore, one can estimate a change of R from a variation of the peak position E relative to the

:

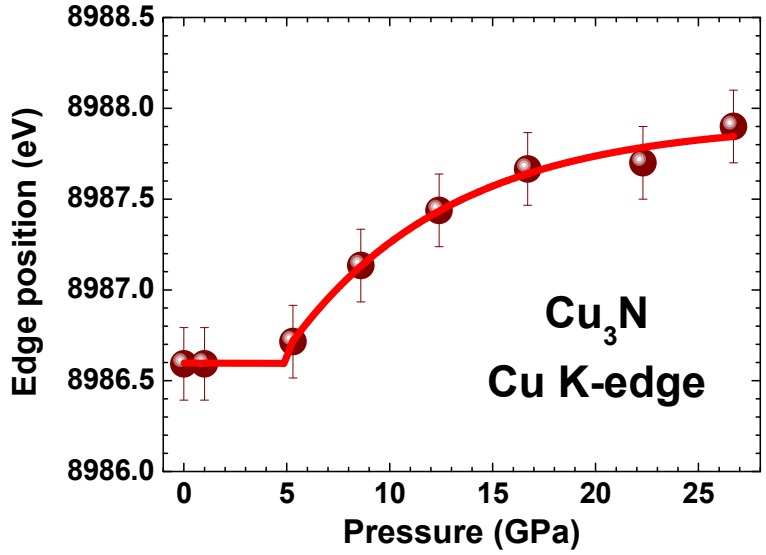

e normalized edge jump (solid circles) at the Cu
/e.

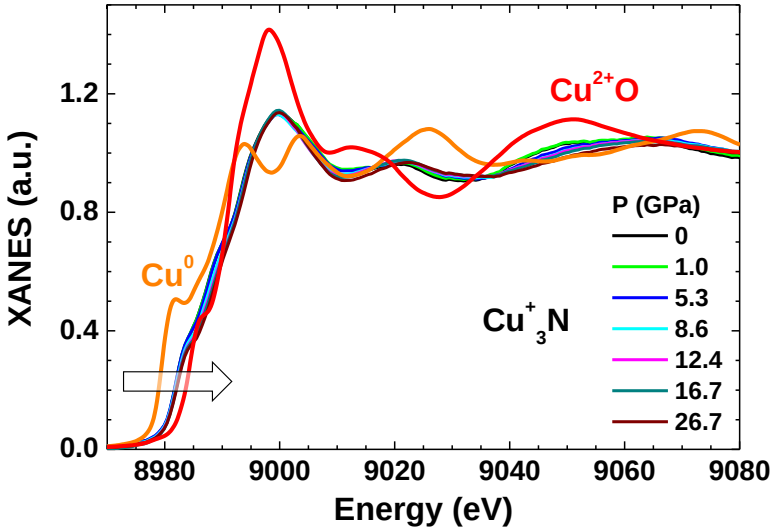

Figure 5 Comparison of the Cu K-edge XANES of Cu_3N, metallic copper and CuO. The data for Cu and CuO are from Ref.[51] .

threshold E_0. This method was successfully used in the past to estimate the metal–oxygen bond length in high-temperature superconductors[53] and manganites.[54,55] A shift of each peak in XANES by ΔE to larger energies corresponds to a decrease of the respective scattering path length by ΔR. We applied Natoli's rule to five peaks observed in the experimental XANES at 9000, 9022, 9065, 9138 and 9201 eV. The results suggest a reduction of the lattice parameter by $\sim$2.3% at 26.7 GPa.

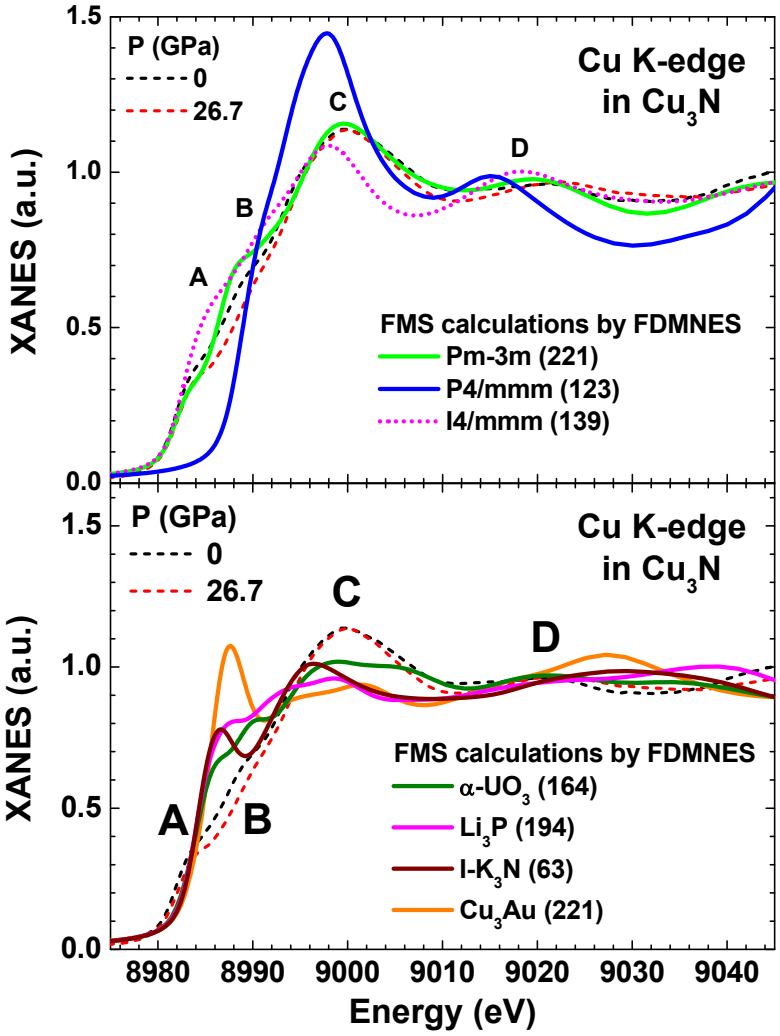

Figure 6 Comparison of the Cu K-edge XANES FMS calculations by FDMNES code for several crystal phases with the experimental XANES of Cu_3N at 0 and 26.7 GPa.

Further support for our XANES results was obtained from the analysis of EXAFS. The experimental Cu K-edge EXAFS spectra $\chi(k)k^2$ and their Fourier transforms are shown in Figure 7. Note that the EXAFS range is strongly limited when measurements are performed in dispersive mode. We obtained good quality experimental data up to $k_{\max} = 7.5$ Å^{-1}. A relatively short k-space range is responsible for the broadening of peaks in the Fourier transforms. The EXAFS spectra at two extreme pressures (0 and 26.7 GPa) are close in shape and differ mainly in frequency. The observed decrease of the frequency of EXAFS oscillations upon increasing pressure suggests a reduction of the lattice parameter and, consequently, a shortening of interatomic distances denoted with the horizontal arrow.

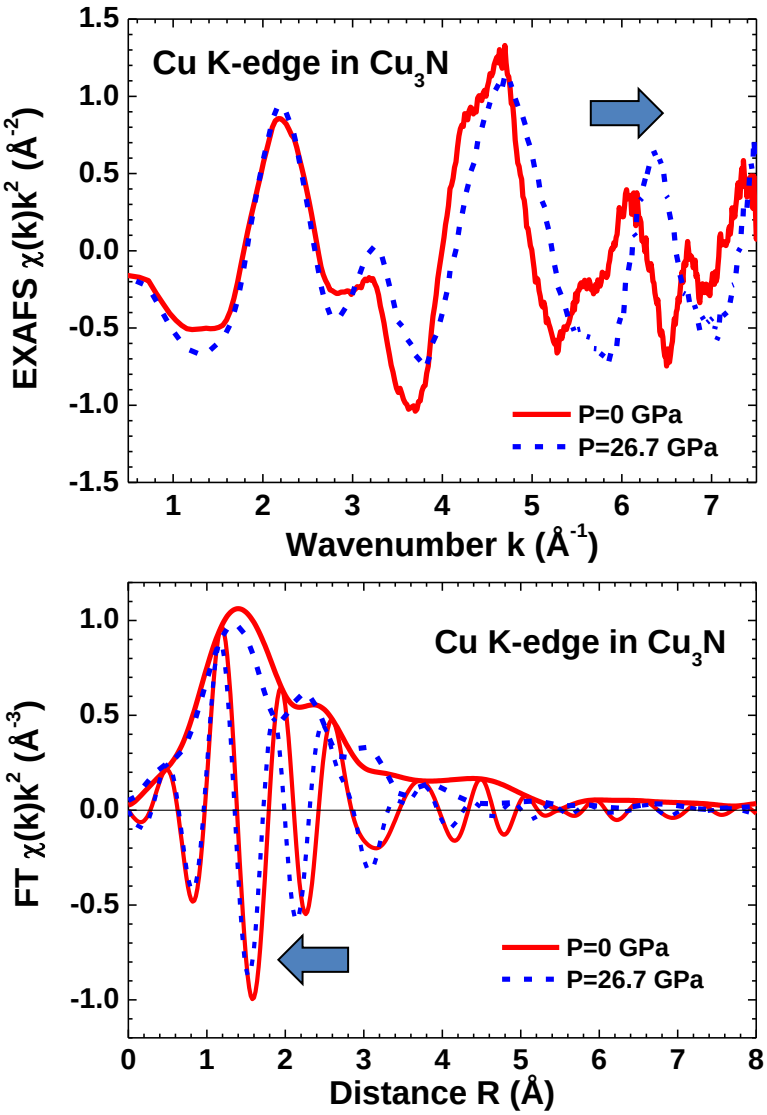

Figure 7 Comparison of the experimental Cu K-edge EXAFS spectra $\chi(k)k^2$ (upper panel) and their Fourier transforms (FTs) (lower panel, modulus and imaginary parts are shown) for Cu_3N at 0 and 26.7 GPa. Note that the peaks in FTs do not appear at the true interatomic distances due to the extra phase shifts.

The EXAFS spectra of Cu_3N were least-square curve fitted within the single-scattering approximation (Figure 8) using a simple model, based on a fragment of the Cu_3N structure with the $Pm\bar{3}m$ symmetry and containing six coordination shells around absorbing copper atom. Note that the first four shells, composed of two nearest nitrogen atoms at ∼1.9 Å, eight copper atoms at ∼2.7 Å, six copper atoms at ∼3.8 Å and eight nitrogen atoms at ∼4.2 Å, produce the main contribution to EXAFS. Our simple model reproduces well main features of the experimental EXAFS spectra at both pressures.

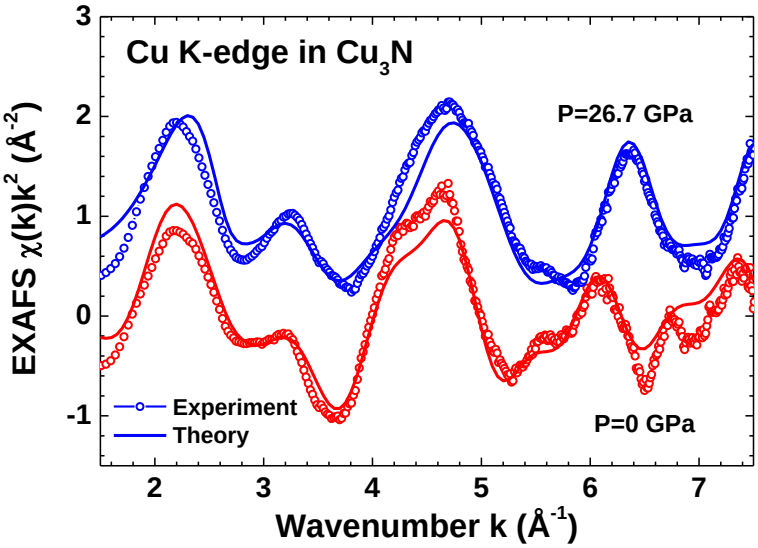

Figure 8 Comparison of the experimental (open circles) and calculated (solid lines) Cu K-edge EXAFS spectra $\chi(k)k^2$ of Cu_3N at 0 and 26.7 GPa.

The values of the lattice parameters $a_0 = 3.82$ Å at 0 GPa and $a_0 = 3.74$ Å at 26.7 GPa, estimated from interatomic distances, suggest the lattice parameter reduction by $\sim$2% upon compression up to 26.7 GPa. This result agree nicely with the previous estimate by Natoli's rule. Thus, one can conclude that the results of EXAFS analysis provide additional support for the stability of cubic $Pm\bar{3}m$ (221) phase in the range of 0–26.7 GPa.

Pressure-dependence of Cu_3N properties was studied in the past by electrical resistance[28] and optical absorption[29] measurements.

It was found[28] that the resistance of Cu_3N is semiconductor-like (about 10^5 Ω) at ambient pressure, drops by about five orders of magnitude in the pressure range of 3–10 GPa, and then remains at several ohms above 10 GPa. Upon releasing pressure back to ambient, the resistance increases slightly remaining in about several ohms range.

The electronic properties of Cu_3N were indirectly probed by measuring optical response in the infrared and visible frequency range.[29] A strong increase of the absorption in the infrared range at 1 eV was found already at 1 GPa because of excitations across the band gap.[50] The absorption in the infrared range strongly increases above 4 GPa and becomes nearly flat above 7 GPa.[29] Note that the

A. Kuzmin, A. Anspoks, A. Kalinko, J. Timoshenko, L. Nataf, F. Baudelet, T. Irifune,
Origin of pressure-induced metallization in Cu3N: an X-ray absorption spectroscopy study,
Phys. Status Solidi B 255 (2018) 1800073:1-6.

initial low absorption level was not recovered upon pressure release, being in good correlation with the behavior of the resistance.[28]

Summarizing both experimental findings[28,29] one can propose three possible models for their explanation: (i) band gap collapse of cubic Cu_3N phase upon compression; (ii) a transition to a different Cu_3N phase; (iii) a transition to metallic copper due to nitrogen loss.

The electronic structure of Cu_3N was studied by first principles calculations in a number of works.[31–33,50,56]

The results of the full-potential linearized augmented plane wave (FP-LAPW) calculations using density functional theory (DFT) predicted a phase transition of Cu_3N at $\sim$17 GPa from cubic $Pm\bar{3}m$ phase to a hypothetic cubic Cu_3Au-type phase, having the same space group (221) but with Cu and N atoms occupying two different Wyckoff positions – 1a (0,0,0) and 3c (0,1/2,1/2), respectively.[31]

Eight structure candidates for high-pressure phases of Cu_3N were investigated in Ref.[32] based on the Hartree-Fock and DFT-B3LYP methods. The obtained results suggested that three phases might be stable at high pressures of about 25–35 GPa: the hexagonal Li_3P-type (194), trigonal α-UO_3-type (164) and orthorhombic I-K_3N-type (63).

Finally, recent FP-LAPW DFT calculations using a modified Becke-Johnson (mBJ) exchange potential approximation proposed that the cubic Cu_3N ($Pm\bar{3}m$ (221)) structure is mechanically most stable under high pressures.[33] The calculations predict that Cu_3N is an indirect band gap (0.6 eV) semiconductor and becomes a metal at 5-10 GPa and a semi-metal at 20-30 GPa.[33]

Experimental high-pressure diffraction studies[29,30] have proposed a transition from cubic $Pm\bar{3}m$ to tetragonal $I4/mmm$ phase at $\sim$8.2 GPa[29] or $\sim$12 GPa.[30] The existence of the intermediate tetragonal $P4/mmm$ phase has been evidenced as well.[30] However, the diffraction patterns of these phases are rather close taking into account the broadening of peaks at high pressure.

Therefore, we propose based on our high-pressure X-ray absorption spectroscopy study and recent first-principles calculations[33] that the cubic ($Pm\bar{3}m$) structure of Cu_3N remains stable at least up to 26.7 GPa. The band gap of Cu_3N decreases upon the lattice compression, and an overlap between conduction and valence bands leads to metallic behavior.

A. Kuzmin, A. Anspoks, A. Kalinko, J. Timoshenko, L. Nataf, F. Baudelet, T. Irifune,
Origin of pressure-induced metallization in Cu3N: an X-ray absorption spectroscopy study,
Phys. Status Solidi B 255 (2018) 1800073:1-6.

5. Conclusion

Cubic Cu_3N with anti-perovskite structure was studied by *in situ* high-pressure X-ray absorption spectroscopy at the Cu K-edge using synchrotron radiation.

The transition to metal state above 5 GPa, observed previously by pressure-dependent electrical resistance[28] and optical absorption[29] measurements, is explained by the band gap collapse due to a decrease of the unit cell volume. The lattice parameter of Cu_3N is reduced by $\sim 2\%$ upon increasing pressure up to 26.7 GPa, nevertheless the structure is restored upon pressure release. At all pressures the local atomic structure of Cu_3N remains close to that in the cubic $Pm\bar{3}m$ phase, supporting its stability.

Acknowledgements The authors are grateful to Professor Alain Polian for providing the NDAC cell. This study was supported by Latvian National Research program IMIS2. The experiment at the SOLEIL synchrotron radiation facility received funding from the European Community's Seventh Framework Programme (FP7/2007-2013) CALIPSO under Grant agreement no. 312284.

Conflict of Interest The authors declare no conflict of interest.

References

[1] F. J. Manjóon, D. Errandonea, *Phys. Status Solidi B* **2009**, *246*, 9.

[2] J. Shu, *Geosci. Front.* **2012**, *3*, 1.

[3] R. J. Hemley, H.-K. Mao, V. V. Struzhkin, *J. Synchrotron Rad.* **2005**, *12*, 135.

[4] G. Shen, H. K. Mao, *Rep. Prog. Phys.* **2017**, *80*, 016101.

[5] B. B. Karki, L. Stixrude, R. M. Wentzcovitch, *Rev. Geophys.* **2001**, *39*, 507.

[6] K. Umemoto, R. M. Wentzcovitch, *Phys. Rev. B* **2006**, *74*, 224105.

[7] Y. Wang, X. Lu, W. Yang, T. Wen, L. Yang, X. Ren, L. Wang, Z. Lin, Y. Zhao, *J. Am. Chem. Soc.* **2015**, *137*, 11144.

[8] B. Lavina, P. Dera, R. T. Downs, *Rev. Mineral. Geochem.* **2014**, *78*, 1.

[9] J. Liu, *Chinese Phys. B* **2016**, *25*, 076106.

[10] S. Pascarelli, O. Mathon, *Phys. Chem. Chem. Phys.* **2010**, *12*, 5535.

[11] D. Andrault, M. Munoz, N. Bolfan-Casanova, N. Guignot, J.-P. Perrillat, G. Aquilanti, S. Pascarelli, *Earth Planet Sci Lett.* **2010**, *293*, 90.

[12] N. Ishimatsu, K. Matsumoto, H. Maruyama, N. Kawamura, M. Mizumaki, H. Sumiya, T. Irifune, *J. Synchrotron Rad.* **2012**, *19*, 768.

[13] Y. Zhao, J. Zhang, *J. Appl. Crystallogr.* **2008**, *41*, 1095.

[14] D. Machon, F. Meersman, M. Wilding, M. Wilson, P. McMillan, *Prog. Mater. Sci.* **2014**, *61*, 216.

[15] M. Asano, K. Umeda, A. Tasaki, *Jap. J. Appl. Phys.* **1990**, *29*, 1985.

[16] R. Cremer, M. Witthaut, D. Neuschütz, C. Trappe, M. Laurenzis, O. Winkler, H. Kurz, *Microchim. Acta*, *133*, 299.

[17] X. Xu, N. Yuan, J. Qiu, J. Ding, *Mater. Res. Bull.* **2015**, *65*, 68.

[18] W. Zhu, X. Zhang, X. Fu, Y. Zhou, S. Luo, X. Wu, *Phys. Status Solidi A* **2012**, *209*, 1996.

[19] Y. Fang, J. Persson, C. Zha, J. Willman, C. W. Miller, J. Åkerman, *J. Appl. Phys.* **2012**, *111*, 073912.

[20] A. Zakutayev, C. M. Caskey, A. N. Fioretti, D. S. Ginley, J. Vidal, V. Stevanovic, E. Tea, S. Lany, *J. Phys. Chem. Lett.* **2014**, *5*, 1117.

[21] T. Nakamura, H. Hayashi, T. Hanaoka, T. Ebina, *Inorg. Chem.* **2014**, *53*, 710.

[22] R. Juza, H. Hahn, *Z. Anorg. Allg. Chem.* **1938**, *239*, 282.

[23] U. Zachwieja, H. Jacobs, *J. Less Common Metals* **1990**, *161*, 175.

[24] Z. Liu, W. Wang, T. Wang, S. Chao, S. Zheng, *Thin Solid Films* **1998**, *325*, 55.

[25] S. Ghosh, F. Singh, D. Choudhary, D. Avasthi, V. Ganesan, P. Shah, A. Gupta, *Surf. Coat. Technol.* **2001**, *142-144*, 1034.

[26] T. Nosaka, M. Yoshitake, A. Okamoto, S. Ogawa, Y. Nakayama, *Appl. Surface Sci.* **2001**, *169-170*, 358.

[27] Y. Du, R. Huang, R. Song, L. B. Ma, C. Liu, C. Li, Z. X. Cao, *J. Mater. Res.* **2007**, *22*, 3052.

[28] J. G. Zhao, L. X. Yang, Y. Yu, S. J. You, J. Liu, C. Q. Jin, *Phys. Stat. Sol. (b)* **2006**, *243*, 573.

[29] A. Wosylus, U. Schwarz, L. Akselrud, M. G. Tucker, M. Hanfland, K. Rabia, C. Kuntscher, J. von Appen, R. Dronskowski, D. Rau, R. Niewa, *Z. Anorg. Allg. Chem.* **2009**, *635*, 1959.

[30] J. Zhao, S. You, L. Yang, C. Jin, *Solid State Commun.* **2010**, *150*, 1521.

A. Kuzmin, A. Anspoks, A. Kalinko, J. Timoshenko, L. Nataf, F. Baudelet, T. Irifune,
Origin of pressure-induced metallization in Cu3N: an X-ray absorption spectroscopy study,
Phys. Status Solidi B 255 (2018) 1800073:1-6.

[31] W. Yu, L. Li, C. Jin, *J. Mater. Sci.* **2005**, *40*, 4661.

[32] Z. Cancarevic, J. C. Schön, M. Jansen, *Z. Anorg. Allg. Chem.* **2005**, *631*, 1167.

[33] M. Ghoohestani, M. Karimipour, Z. Javdani, *Phys. Scr.* **2014**, *89*, 035801.

[34] J. Timoshenko, A. Anspoks, A. Kalinko, A. Kuzmin, *Phys. Scr.* **2016**, *91*, 054003.

[35] A. Kuzmin, A. Kalinko, A. Anspoks, J. Timoshenko, R. Kalendarev, *Latvian J. Phys. Tech. Sci.* **2016**, *53*, 31.

[36] J. Timoshenko, A. Anspoks, A. Kalinko, A. Kuzmin, *Acta Mater.* **2017**, *129*, 61.

[37] F. Baudelet, Q. Kong, L. Nataf, J. D. Cafun, A. Congeduti, A. Monza, S. Chagnot, J. P. Itié, *High Press. Res.* **2011**, *31*, 136.

[38] I. Tetsuo, K. Ayako, S. Shizue, I. Toru, S. Hitoshi, *Nature* **2003**, *421*, 599.

[39] P. I. Dorogokupets, A. R. Oganov, *Phys. Rev. B* **2007**, *75*, 024115.

[40] N. Doebelin, R. Kleeberg, *J. Appl. Crystallogr.* **2015**, *48*, 1573.

[41] A. Kuzmin, *Physica B* **1995**, *208-209*, 175.

[42] A. Kuzmin, J. Chaboy, *IUCrJ* **2014**, *1*, 571.

[43] Y. Joly, *Phys. Rev. B* **2001**, *63*, 125120.

[44] O. Bunău, Y. Joly, *J. Phys.: Condensed Matter* **2009**, *21*, 345501.

[45] L. Hedin, S. Lundqvist, *J. Phys. C: Solid State Phys.* **1971**, *4*, 2064.

[46] U. von Barth, L. Hedin, *J. Phys. C: Solid State Phys.* **1972**, *5*, 1629.

[47] J. J. Rehr, R. C. Albers, *Rev. Mod. Phys.* **2000**, *72*, 621.

[48] J. J. Rehr, J. J. Kas, F. D. Vila, M. P. Prange, K. Jorissen, *Phys. Chem. Chem. Phys.* **2010**, *12*, 5503.

[49] G. Paniconi, Z. Stoeva, H. Doberstein, R. I. Smith, B. L. Gallagher, D. H. Gregory, *Solid State Sci.* **2007**, *9*, 907.

[50] U. Hahn, W. Weber, *Phys. Rev. B* **1996**, *53*, 12684.

[51] A. Kuzmin, A. Anspoks, A. Kalinko, J. Timoshenko, R. Kalendarev, *J. Non-Cryst. Solids* **2014**, *401*, 87.

[52] C. R. Natoli, in *EXAFS and Near Edge Structure*, ed. A. Bianconi, L. Incoccia, S. Stipcich, Springer-Verlag, Berlin, 1983, p. 43.

A. Kuzmin, A. Anspoks, A. Kalinko, J. Timoshenko, L. Nataf, F. Baudelet, T. Irifune,
Origin of pressure-induced metallization in Cu3N: an X-ray absorption spectroscopy study,
Phys. Status Solidi B 255 (2018) 1800073:1-6.

[53] H. Tolentino, F. Baudelet, A. Fontaine, T. Gourieux, G. Krill, J. Henry, J. Rossat-Mignod, *Physica C* **1992**, *192*, 115.

[54] N. M. Souza-Neto, A. Y. Ramos, H. C. N. Tolentino, E. Favre-Nicolin, L. Ranno, *Phys. Rev. B* **2004**, *70*, 174451.

[55] D. M. A. Melo, F. M. M. Borges, R. C. Ambrosio, P. M. Pimentel, C. N. da Silva Junior, M. A. Melo, *Chem. Phys.* **2006**, *322*, 477.

[56] M. G. Moreno-Armenta, A. Martínez-Ruiz, N. Takeuchi, *Solid State Sci.* **2004**, *6*, 9.

A. Kuzmin, A. Anspoks, A. Kalinko, J. Timoshenko, L. Nataf, F. Baudelet, T. Irifune,
Origin of pressure-induced metallization in Cu3N: an X-ray absorption spectroscopy study,
Phys. Status Solidi B 255 (2018) 1800073:1-6.

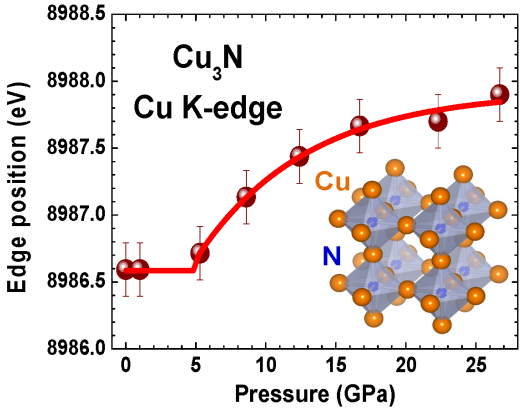

Origin of pressure-induced metallization in cubic Cu_3N has been disclosed using *in situ* Cu K-edge X-ray absorption spectroscopy. The transition to metal state above 5 GPa is explained by the band gap collapse due to a decrease of the unit cell volume. The lattice parameter of Cu_3N is reduced by $\sim 2\%$ upon increasing pressure up to 26.7 GPa, and the structure is restored upon pressure release. The local atomic structure of Cu_3N remains close to that in cubic $Pm\bar{3}m$ at all pressures.

Graphical Table of Contents

Institute of Solid State Physics, University of Latvia as the Center of Excellence has received funding from the European Union's Horizon 2020 Framework Programme H2020-WIDESPREAD-01-2016-2017-TeamingPhase2 under grant agreement No. 739508, project CAMART²